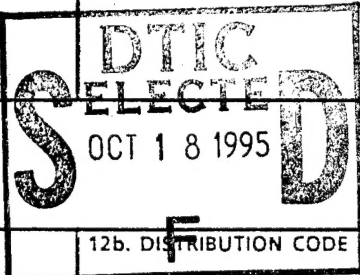


REPORT DOCUMENTATION PAGE			Form Approved OMB No. 0704-0188	
Public reporting burden for this collection of information is estimated to average 1 hour per response, including the time for reviewing instructions, searching existing data sources, gathering and maintaining the data needed, and completing and reviewing the collection of information. Send comments regarding this burden estimate or any other aspect of this collection of information, including suggestions for reducing this burden, to Washington Headquarters Services, Directorate for Information Operations and Reports, 1215 Jefferson Davis Highway, Suite 1204, Arlington, VA 22202-4302, and to the Office of Management and Budget, Paperwork Reduction Project (0704-0188), Washington, DC 20503.				
1. AGENCY USE ONLY (Leave blank)		2. REPORT DATE 10 Sep 95		3. REPORT TYPE AND DATES COVERED
4. TITLE AND SUBTITLE Refinement of a Semi-Empirical Model for the Microwave Emissivity of the Sea Surface as a Function of Wind Speed			5. FUNDING NUMBERS	
6. AUTHOR(S) David Jacob Kohn				
7. PERFORMING ORGANIZATION NAME(S) AND ADDRESS(ES) AFIT Students Attending:  Texas A&M University			8. PERFORMING ORGANIZATION REPORT NUMBER  95-090	
9. SPONSORING/MONITORING AGENCY NAME(S) AND ADDRESS(ES) DEPARTMENT OF THE AIR FORCE AFIT/CI 2950 P STREET, BLDG 125 WRIGHT-PATTERSON AFB OH 45433-7765			10. SPONSORING/MONITORING AGENCY REPORT NUMBER	
11. SUPPLEMENTARY NOTES				
12a. DISTRIBUTION/AVAILABILITY STATEMENT Approved for Public Release IAW AFR 190-1 Distribution Unlimited BRIAN D. GAUTHIER, MSgt, USAF Chief of Administration				
12b. DISTRIBUTION CODE				
13. ABSTRACT (Maximum 200 words)				
<p style="font-size: 2em; margin: 0;">19951017 146</p> <p style="margin: 0;">DTIC QUALITY INSPECTED 8</p>				
14. SUBJECT TERMS			15. NUMBER OF PAGES 44	
			16. PRICE CODE	
17. SECURITY CLASSIFICATION OF REPORT	18. SECURITY CLASSIFICATION OF THIS PAGE	19. SECURITY CLASSIFICATION OF ABSTRACT	20. LIMITATION OF ABSTRACT	

**REFINEMENT OF A SEMI-EMPIRICAL MODEL FOR THE MICROWAVE  
EMISSION OF THE SEA SURFACE AS A FUNCTION OF WIND SPEED**

A Thesis

by

DAVID JACOB KOHN

Submitted to the Office of Graduate Studies of  
Texas A&M University  
in partial fulfillment of the requirements for the degree of

MASTER OF SCIENCE

Accession For	
NTIS CRA&I	<input checked="" type="checkbox"/>
DTIC TAB	<input type="checkbox"/>
Unannounced	<input type="checkbox"/>
Justification	
By	
Distribution /	
Availability Codes	
Dist	Avail and/or Special
A-1	

December 1995

Major Subject: Meteorology

**REFINEMENT OF A SEMI-EMPIRICAL MODEL FOR THE MICROWAVE  
EMISSION OF THE SEA SURFACE AS A FUNCTION OF WIND SPEED**

A Thesis

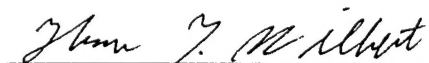
by

DAVID JACOB KOHN

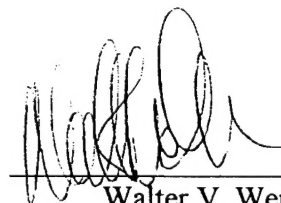
Submitted to the Office of Graduate Studies of  
Texas A&M University  
in partial fulfillment of the requirements for the degree of

MASTER OF SCIENCE

Approved as to style and content by:



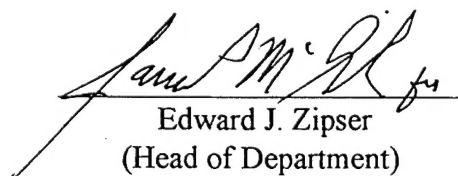
Thomas T. Wilheit  
(Chair of Committee)



Walter V. Wendler  
(Member)



Gerald R. North  
(Member)



Edward J. Zipser  
(Head of Department)

December 1995

Major Subject: Meteorology

## ABSTRACT

Refinement of a Semi-Empirical Model for the Microwave Emissivity of  
the Sea Surface as a Function of Wind Speed. (December 1995)

David Jacob Kohn, B.S., Michigan Technological University

Chair of Advisory Committee: Dr. Thomas T. Wilheit

In 1979, Wilheit introduced a sea surface emissivity model for microwave frequencies. This model is used in a radiative transfer model (RTM) to obtain simulated brightness temperatures for various atmospheric conditions. The brightness temperatures are used to obtain algorithms for atmospheric variables. These algorithms can then be used to retrieve atmospheric variables from the microwave measurements. Therefore, it is important to get the surface emissivity right.

Several changes are made to Wilheit's sea surface emissivity model. The first change to the model is to the model's treatment of multiple reflections. Multiple reflections are now treated as if the radiation is reflected back into the view path of the microwave sensor. This change lowered the computed emissivity of the sea surface; which is more representative of observations without sea foam. The second change is made to the sea surface roughness parameter. An increase in roughness is needed at frequencies above 16.6 GHz and a decrease below 16.6 GHz. The roughness is increased to 132% of the Cox and Munk roughness at 37 GHz and 30% of the roughness at 6.6 GHz. The last change to the model is in the treatment of sea foam. The foam effect is now a smooth transition of increasing foam as the wind speed increases; instead of being switched on at 7 m/s. These

changes yield an improved sea surface model that is within 2% of the sea surface emissivity given by the Wentz sea surface emissivity functions.

## ACKNOWLEDGMENTS

I would like to thank Dr. Wilheit for his guidance and patience throughout my research. He kept me focused and his helpful critiques of my work enabled me to complete my research in a timely manner. I give thanks to Dr. North and Dr. Wendler for taking time out of their schedule to be on my committee. From the Microwave Research Group, I want to give special thanks to Clay Blankenship and Jeff Tesmer for their insights and help on my research and to all the other members of the research group, thanks for your support. I also want to thank John Polander for his help and encouragement to complete my research.

Finally, I would like to thank my wife, Lara, for her understanding and a kick in the rear to get me going when I had all but given up. Also thanks to my new born son, Matthew, for doing without a father for the last several months.

Funding for my education and the bulk of my research was provided by the United States Air Force and was partially supported by NASA contract number NAS5-3259.

THANKS !

**TABLE OF CONTENTS**

	Page
ABSTRACT.....	iii
ACKNOWLEDGMENTS.....	v
TABLE OF CONTENTS.....	vi
LIST OF FIGURES.....	vii
LIST OF TABLES.....	viii
1. INTRODUCTION.....	1
2. DESCRIPTION OF THE SEA SURFACE EMISSIVITY FUNCTIONS AND MODEL.....	4
a. Scanning Multichannel Microwave Radiometer (SMMR).....	4
b. Special Sensor Microwave Imager (SSM/I).....	8
c. Sea Surface Emissivity Model.....	10
3. REFINEMENT AND COMPARISON.....	14
4. CONCLUSION.....	37
REFERENCES.....	38
APPENDIX A.....	40
VITA.....	44

# LIST OF FIGURES

FIGURE		Page
1	Two component radiative transfer model.....	3
2	Incidence angle dependence of the model and the SSM/I function for surface emissivity.....	16
3	The sea surface temperature dependence of the sea surface emissivity model.....	17
4	Wind speed dependence of the model and the SSM/I function.....	18
5	The treatment of multiple reflections in the model.....	19
6	Plots of the roughness parameter for SMMR frequencies.....	21
7	A comparison of Hollinger's and the new model's Cox and Munk variance adjustment.....	22
8	Plots of the roughness parameter for SMMR frequencies after the variance adjustment.....	24
9	Total foam effect.....	25
10	Adjusted foam effect with zero foam at 0 m/s wind speed.....	26
11	Wind speed dependence of the foam effect.....	28
12	The remaining foam contribution after the base function is subtracted from the total foam effect.....	29
13	The remaining foam contribution expressed as a fraction of the base function.....	30
14	A comparison of the 37 GHz emissivities from the SMMR and SSM/I functions.....	32
15	Frequency dependence of the foam effect at 20 m/s wind speed.....	35
16	Emissivities from the new model and the Wentz functions.....	36



**LIST OF TABLES**

TABLE		Page
1	Regression coefficients for smooth surface brightness temperature.....	6
2	Wind induced emissivity coefficients.....	7
3	Coefficients for the smooth surface emissivity expression at the SSM/I channels.....	9
4	Coefficients for the frequency dependence equations of the foam effect.....	33

## 1. INTRODUCTION

Surface observations are needed to initialize forecast models. As forecast models become more sophisticated, accuracy and increased spatial resolution of observations become more important. Since the majority of the earth's surface is ocean, a large part of the earth is not covered by surface observations. These observations are needed for an accurate initialization field in forecast models. Satellite remote sensing can provide the necessary atmospheric parameters over the ocean to fill this gap in the surface observation network.

The Multi-frequency Imaging Microwave Radiometer (MIMR), a passive microwave sensor, is planned to be launched in the year 2000. One will be able to retrieve general atmospheric parameters from the MIMR frequencies. A radiative transfer model (RTM) will be used to simulate the expected brightness temperatures in various atmospheres for the MIMR frequencies. These simulated brightness temperatures will be regressed against the various atmospheric parameters to obtain operational algorithms.

Currently, the Special Sensor Microwave/Imager (SSM/I) is a remote sensing instrument used for data collection. The SSM/I is flown on polar orbiting satellites and has global coverage approximately twice daily. This sensor measures upwelling radiation from the earth's surface. However, a uniform reflective surface is needed to make accurate inferences of atmospheric variables. Therefore, for many parameters the only useful data are collected over oceanic areas.

---

The journal model for this thesis is the *Journal of Applied Meteorology*.

The SSM/I radiances are reported as brightness temperatures. Brightness temperatures are measured in the horizontal and vertical polarizations at 19.35, 37.0, and 85.5 GHz. The 22.235 GHz channel measures only the vertical polarization. Brightness temperatures are a combination of surface emission, upward radiation by atmospheric constituents, and downward emission and cosmic background radiation reflected off the sea surface (Fig. 1). Various geophysical parameters; cloud liquid water (CLW), precipitable water (PW), and sea surface wind speed (WS); can be retrieved from combinations of brightness temperatures. Also, sea surface temperatures (SST) are needed to initialize the forecast models which cannot be obtained from the SSM/I frequencies. However, the MIMR having additional frequencies will provide all the above parameters.

An integral part of the RTM is the sea surface emissivity calculation. Wind roughens the sea surface and produces foam. This roughness and foam cause changes in sea surface emissivity and therefore in the radiances. Wentz has developed two empirical sea surface emissivity functions. He developed one for the scanning multichannel microwave radiometer (SMMR) frequencies and the other for the SSM/I frequencies. Although, these functions work well at describing the surface emissivity, they are limited to the frequencies and incidence angles for which they were developed. A general model for the surface emissivities is needed to be able to simulate brightness temperatures at other frequencies and incidence angles. The objective of this research is to refine the surface emissivity model to better reflect the relationship between wind speed and sea surface emissivity.

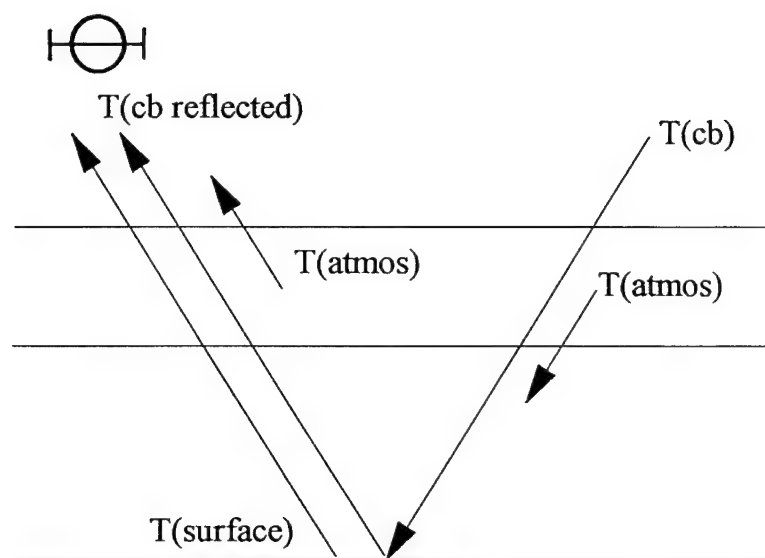


Fig. 1. Two component (single layer atmosphere and surface) radiative transfer model.

## 2. DESCRIPTION OF THE SEA SURFACE EMISSIVITY

### FUNCTIONS AND MODEL

#### *a. Scanning multichannel microwave radiometer (SMMR)*

From the scanning multichannel microwave radiometer (SMMR) sensor data, Wentz (1983) developed an expression to retrieve sea surface emissivity. He separated the sea surface emissivity into two parts. The first part is the contribution from a smooth sea surface. The second part is the contribution from wind induced roughness and foam. The total emissivity ( $E$ ) can be written as

$$E = E_s + E_r \quad (1)$$

where  $E_s$  is the smooth surface emissivity and  $E_r$  is the rough surface and foam part of the emissivity.

The smooth surface contribution to emissivity is computed from the dielectric constant of sea water in conjunction with the Fresnel relations (Smith 1988). Klein and Swift (1977) reviewed experimental data, in the 1 to 4 GHz range, and derived an expression for the dielectric constant of sea water as a function of temperature, salinity, conductivity, frequency, and polarization. Wentz (1983) used this function for the dielectric constant and the Fresnel relation to derive an expression for  $E_s$ . The resulting expression follows

$$E_s = \frac{S_0 + S_1 T + S_2 T^2 + S_3 T^3 + S_4 (\theta_i - 49^\circ)}{T_s} \quad (2)$$

where

$$T = T_s - 273.16 \quad (3)$$

and  $T_s$  is the surface temperature in Kelvin (K). This expression only applies to incidence angles of  $49^\circ \pm 0.5^\circ$ . The coefficients for the expression at SMMR frequencies are in Table 1. These coefficients were found by using a least squares fit to the available data (Wentz 1983).

After subtracting the brightness temperature ( $T_b$ ) attributed to the smooth surface effect from the SMMR data, the remainder is considered to be due to a wind roughened sea surface and sea foam. The amount of roughening, as the wind blows across the sea surface, is related to the friction velocity ( $u_*$ ) (Ross and Cardone 1974). In an unstable boundary layer, cold air over warm water, there is more wind stress ( $u_*$ ) for a given wind speed at a height over the water than in a neutral or stable boundary layer. The remaining brightness temperature is regressed with  $u_*$  to derive an expression for the rough surface and foam contribution to the emissivity as a function of  $u_*$  (Wentz 1983). Wentz *et al.* (1986) revised the  $u_*$  relation to one that uses wind speed in m/s at 19.5 meters. The new expressions for the rough surface and foam contribution ( $E_r$ ) to the emissivity are

$$E_r = m_1 WS \quad WS \leq 7 \text{ m/s} \quad (4)$$

$$E_r = m_1 WS + 0.05(m_2 - m_1)(WS - 7)^2 \quad 7 < WS < 17 \text{ m/s} \quad (5)$$

$$E_r = m_2 WS - 12(m_2 - m_1) \quad WS \geq 17 \text{ m/s} \quad (6)$$

where WS is the wind speed. The  $m$  coefficients are in Table 2. The coefficients were found by a least squares fit to the residuals of the brightness temperature (Wentz *et al.* 1986).

TABLE 1. Regression coefficients for smooth surface brightness temperature (Wentz 1983).

SMMR Channel	$S_0$ (K)	$S_1$	$S_2$ (K <sup>-1</sup> )	$S_3$ (K <sup>-2</sup> )	$S_4$ (K/deg)
6.6 V	$1.3759 \times 10^2$	$2.368 \times 10^{-1}$	$1.565 \times 10^{-2}$	$-2.311 \times 10^{-4}$	2.03
6.6 H	$0.7107 \times 10^2$	$0.891 \times 10^{-1}$	$1.000 \times 10^{-2}$	$-2.497 \times 10^{-4}$	-1.28
10.7 V	$1.4452 \times 10^2$	$-0.336 \times 10^{-1}$	$2.076 \times 10^{-2}$	$-2.497 \times 10^{-4}$	2.05
10.7 H	$0.7559 \times 10^2$	$-0.935 \times 10^{-1}$	$1.371 \times 10^{-2}$	$-1.661 \times 10^{-4}$	-1.32
18 V	$1.5750 \times 10^2$	$-3.936 \times 10^{-1}$	$2.285 \times 10^{-2}$	$-2.048 \times 10^{-4}$	2.08
18 H	$0.8444 \times 10^2$	$-3.675 \times 10^{-1}$	$1.675 \times 10^{-2}$	$-1.568 \times 10^{-4}$	-1.40
21 V	$1.6252 \times 10^2$	$-4.916 \times 10^{-1}$	$2.237 \times 10^{-2}$	$-1.775 \times 10^{-4}$	2.10
21 H	$0.8802 \times 10^2$	$-4.546 \times 10^{-1}$	$1.699 \times 10^{-2}$	$-1.477 \times 10^{-4}$	-1.43
37 V	$1.8493 \times 10^2$	$-7.405 \times 10^{-1}$	$1.694 \times 10^{-2}$	$-0.539 \times 10^{-4}$	2.11
37 H	$1.0524 \times 10^2$	$-7.666 \times 10^{-1}$	$1.718 \times 10^{-2}$	$-1.033 \times 10^{-4}$	-1.59

TABLE 2. Wind induced emissivity coefficients (Wentz *et al.* 1986).

Channel	$m_1$ (s/m)	$m_2$ (s/m)
6.6 V	$4.82 \times 10^{-4}$	$34.07 \times 10^{-4}$
6.6 H	$14.28 \times 10^{-4}$	$44.85 \times 10^{-4}$
10.7 V	$6.04 \times 10^{-4}$	$37.32 \times 10^{-4}$
10.7 H	$18.10 \times 10^{-4}$	$54.76 \times 10^{-4}$
18 V	$6.17 \times 10^{-4}$	$35.36 \times 10^{-4}$
18 H	$22.06 \times 10^{-4}$	$60.58 \times 10^{-4}$
21 V	$6.30 \times 10^{-4}$	$33.72 \times 10^{-4}$
21 H	$24.55 \times 10^{-4}$	$61.01 \times 10^{-4}$
37 V	$7.00 \times 10^{-4}$	$25.00 \times 10^{-4}$
37 H	$37.82 \times 10^{-4}$	$63.27 \times 10^{-4}$



*b. Special sensor microwave imager (SSM/I)*

Wentz (1992) also developed an expression for sea surface emissivity using SSM/I frequencies which is similar to his SMMR sea surface emissivity expression. Wentz' SSM/I sea surface emissivity function can be summarized as:

$$E = E_s + E_r + \beta WS(\theta_i - 49^\circ) \quad (7)$$

where  $E_s$  is the smooth surface emissivity,  $E_r$  is the rough surface and foam contribution to the total emissivity,  $WS$  is wind speed (m/s) and  $\theta_i$  is the incidence angle. The third term on the right in equation (7) is the incidence angle dependence of the roughness term. The  $\beta$  coefficient in this term contains a scaling factor between  $u_*$  and wind speed at 19.5 meters. The  $\beta$  coefficient for the five low frequency channels of the SSM/I are in Table 3 (Wentz 1992).

As with the SMMR,  $E_s$  for the SSM/I frequencies are computed using the Klein and Swift (1977) equation for the dielectric constant of sea water and the Fresnel relations (Smith 1988). The new  $E_s$  relation is valid for incidence angles of  $51^\circ \pm 3^\circ$ . The expression for  $E_s$  at the five lower SSM/I frequencies is

$$E_s = \frac{S_0 + S_1 t + S_2 t^2 + S_3 t^3 + S_4 q + S_5 t q + S_6 q^2 + S_7 t^2 q}{T_s} \quad (8)$$

where

$$t = T_s - 273.16 \quad (9)$$

$$q = \theta_i - 51^\circ \quad (10)$$

and  $T_s$  is the sea surface temperature. The values for the  $S$  coefficients are in Table 3 (Wentz 1992).

TABLE 3. Coefficients for the smooth surface emissivity ( $E_s$ ) expression at the SSM/I channels (Wentz 1992).

Coeff.	Units	19 V	19 H	22 V	37 V	37 H
$S_0$	K	$1.6253 \times 10^2$	$0.8220 \times 10^2$	$1.6699 \times 10^2$	$1.8631 \times 10^2$	$0.9974 \times 10^2$
$S_1$	none	$-2.570 \times 10^{-1}$	$-2.805 \times 10^{-1}$	$-3.408 \times 10^{-1}$	$-5.637 \times 10^{-1}$	$-6.171 \times 10^{-1}$
$S_2$	$K^{-1}$	$1.729 \times 10^{-2}$	$1.237 \times 10^{-2}$	$1.735 \times 10^{-2}$	$1.481 \times 10^{-2}$	$1.437 \times 10^{-2}$
$S_3$	$K^{-2}$	$-1.177 \times 10^{-4}$	$-0.925 \times 10^{-4}$	$-1.036 \times 10^{-4}$	$-0.296 \times 10^{-4}$	$-0.707 \times 10^{-4}$
$S_4$	K/deg	2.162	-1.472	2.164	2.123	-1.701
$S_5$	deg $^{-1}$	$0.70 \times 10^{-2}$	$0.21 \times 10^{-2}$	$0.75 \times 10^{-2}$	$1.17 \times 10^{-2}$	$0.55 \times 10^{-2}$
$S_6$	K/deg $^2$	$4.5 \times 10^{-2}$	$-1.6 \times 10^{-2}$	$4.5 \times 10^{-2}$	$4.1 \times 10^{-2}$	$-1.9 \times 10^{-2}$
$S_7$	$K^{-1} \text{deg}^{-1}$	$0.14 \times 10^{-4}$	$-1.10 \times 10^{-4}$	$0.02 \times 10^{-4}$	$-0.71 \times 10^{-4}$	$-1.27 \times 10^{-4}$
$\omega$	s/m	$4.89 \times 10^{-3}$	$9.68 \times 10^{-3}$	$3.78 \times 10^{-3}$	$3.52 \times 10^{-3}$	$8.55 \times 10^{-3}$
$m_1$	s/m	$0.623 \times 10^{-3}$	$2.340 \times 10^{-3}$	$0.634 \times 10^{-3}$	$0.700 \times 10^{-3}$	$4.100 \times 10^{-3}$
$m_2$	s/m	$3.462 \times 10^{-3}$	$6.146 \times 10^{-3}$	$3.305 \times 10^{-3}$	$2.500 \times 10^{-3}$	$7.300 \times 10^{-3}$
$\beta$	s/m deg	$-0.812 \times 10^{-4}$	$0.806 \times 10^{-4}$	$-0.868 \times 10^{-4}$	$-1.193 \times 10^{-4}$	$1.052 \times 10^{-4}$

Next, the contribution by the roughened sea surface and sea foam to the total sea surface emissivity is calculated. The brightness temperature due to the smooth surface and the incidence angle dependence of the roughness term (third term in equation (7)) was subtracted from the total brightness temperature. Then the residual brightness temperatures are fitted by least squares means to get a best fit equation for the rough surface contribution to the total emissivity. The resulting expressions are

$$E_r = m_1 WS \quad WS \leq 7m/s \quad (11)$$

$$E_r = m_1 WS + \frac{(m_2 - m_1)(WS - 7)^2}{20} \quad 7 < WS \leq 17m/s \quad (12)$$

$$E_r = m_2 WS - 12(m_2 - m_1) \quad 17 < WS \quad (13)$$

The  $m$  coefficients are in Table 3 (Wentz 1992).

### *c. Sea surface emissivity model*

Wilheit developed a physically based sea surface emissivity model. Where the sea surface emissivity is a combination of the emissivity given by an ensemble of flat facets and the reduction of the reflectivity of the facets due to a layer of absorbing nonpolarized foam (Wilheit 1979).

Lane and Saxton (1952) did several experiments to determine the dielectric constant of salt water with varying degrees of salinity in a temperature range of -10 to 15°C and a frequency range of 9 to 48 GHz. Using the experimental results of Lane and Saxton's work in conjunction with the Fresnel relations, sea surface emissivity is computed in Wilheit's model (Wilheit 1979).

Wilheit's model does not compute the smooth surface component of the surface emissivity separately from the rough surface component as in the Wentz functions. Rather, the model treats the sea surface as an ensemble of facets (Cox and Munk 1955). Cox and Munk have shown, from sun glint patterns at known wind speeds, that the distribution of facet slopes is Gaussian. The distribution that they used is expressed as

$$P(Z_z, Z_y) = \frac{1}{(\pi\sigma^2)} \exp \left( \frac{-(Z_z^2 + Z_y^2)}{\sigma^2} \right) \quad (14)$$

where  $\sigma^2$  is the variance of the facet slopes. There is a factor of 2 missing in the denominator of the term in front of the exponential term and in the exponential term, which is present in the modern definition of a normal distribution. This is, however, the form used by Cox and Munk. The distribution without the factor of 2 is narrower than one with the factor of 2. The mean square slope of the facets increases as the wind speed increases, so that  $\sigma^2$  be written as a function of wind speed as follows:

$$\sigma^2 = 0.003 + 5.12 \times 10^{-3} WS \pm 0.004 \quad (15)$$

Wind speed (WS) is at 12.5 meters above the surface (Cox and Munk 1955). The Wilheit model makes a slight adjustment in the variance to account for a different wind speed height of 19.5 meters. The variance in the model is given by the expression (Wilheit 1979)

$$\sigma^2 = 0.003 + 4.8 \times 10^{-3} WS \quad (16)$$

This variance of the sea surface roughness leads to an overestimate of the roughness at microwave frequencies (Hollinger 1971). From measurements of wind speed and

microwave brightness temperatures, Hollinger found that at 1.41, 8.36, and 19.34 GHz the variance is approximately 1/3, 1/2, and 2/3 of the Cox and Munk variance respectively. Wilheit found that above 35 GHz the full Cox and Munk variance should be used. To take these findings into account, Wilheit's surface emissivity model adjusts the Cox and Munk variance as follows:

$$\sigma^2(f) = (0.3 + 0.02f)\sigma_{cm}^2 \quad f < 35\text{GHz} \quad (17)$$

$$\sigma^2(f) = \sigma_{cm}^2 \quad f \geq 35\text{GHz} \quad (18)$$

where  $\sigma_{cm}^2$  is the Cox and Munk variance and  $f$  is frequency in GHz (Wilheit 1979).

Having described the sea surface as a Gaussian distribution of facets, the model calculates the surface emissivity as a summation of each facet's emissivity. Each facet's emissivity is calculated by using an equation derived from Lane and Saxton's dielectric constant data and the Fresnel relation; with each facet being treated as a flat (smooth) surface at a different incidence angle.

Once the surface emissivity is calculated, the model takes the sea foam effect into account. Sea foam increases the radiance seen by the sensor. The increase in sea surface emissivity is from 0.37 to 0.6-0.8 at 10 GHz (Williams 1971). During an experiment over the North Atlantic, Nordberg *et al.* (1971) showed that changes in brightness temperature increase linearly with wind speeds above 7 m/s. The amount that foam affects the emissivity is a function of frequency and proportional to wind speed above 7 m/s (Wilheit 1979). The model decreases surface reflectivity due to foam by

$$E_f \cong a \left( 1 - \exp \left( \frac{f}{f_o} \right) \right) (WS - 7) \quad WS > 7\text{m/s} \quad (19)$$

$$E_f = 0 \qquad WS \leq 7m/s \qquad (20)$$

where  $a=0.006$  s/m, and  $f_o=7.5$  GHz. This function is the best fit to the experimental data provided by Webster *et al.* (1976) and Shutko (1978).

### 3. REFINEMENT AND COMPARISON

A better model for the sea surface emissivity is needed to investigate which frequencies will produce the best set of brightness temperatures to be able to retrieve the atmospheric variables. The two existing Wentz functions for surface emissivities are a best fit to available data. They have some residual errors and are not totally self-consistent. The actual values of the functions may not be the same, but the form of the output is consistent. Therefore, the changes to Wilheit's model will have the same form of the Wentz functions but not necessarily the same values.

Several changes are made to Wilheit's sea surface emissivity model. The first change is to the model's treatment of multiple reflections. The second change is made to the sea surface roughness parameter. Finally, the last change is in the treatment of sea foam.

The following variables are held constant during the process of refining Wilheit's sea surface emissivity model. An arbitrary sea surface temperature of 290 K is chosen. The SMMR sea surface emissivity function uses a fixed incidence angle of  $49^\circ$ . Therefore, a fixed incidence angle of  $49^\circ$  is used. Finally, the wind speed ranged from 0 to 40 m/s. These variables stay constant throughout the research unless otherwise specified.

The first comparison between the model and the Wentz SSM/I function for sea surface emissivity is the angle dependence of the emissivity. This comparison was only accomplished for the SSM/I function because the SMMR function is only valid at a fixed incidence angle. The SSM/I function is valid for the incidence angle range of  $48^\circ$  to  $54^\circ$ . The incidence angle is varied between  $45^\circ$  and  $55^\circ$ . The model's incidence angle

dependence followed the Wentz function for surface emissivity (see Fig. 2). Therefore, the model handles the incidence angles correctly.

The model also handled sea surface temperatures correctly. In Fig. 3, it is seen that emissivity decreases with increasing sea surface temperature. This is the same pattern that would result from the Wentz functions because of the  $1/T_s$  relationship in  $E_s$  (see Equations (2) and (8)).

Next, the wind speed dependence of the model is compared to the Wentz functions. As wind speed increases, the model's emissivity departs more from the emissivity given by the Wentz functions (see Fig. 4). The sharp increase in emissivity after 7 m/s is because at this wind speed the model turns on the foam effect. Also, the Wentz function shows a continuous increase in emissivity but the model tends to decrease the emissivity in the vertical polarization until the foam effect starts. The decrease in the model emissivity between 0 and 7 m/s is because the foam effect does not start until 7 m/s. In the real atmosphere there is a smooth transition to increasing foam that starts below 7 m/s. This is best seen in the 37 vertical channel (see Fig. 4).

The way that the model handles multiple reflections is adjusted first because it affects the roughness. In the original model, all multiple reflections are absorbed. This yields a much higher emissivity than is given by the Wentz' sea surface emissivity functions (see Fig. 4). One would expect that some of the background radiation would go through multiple reflections and still be seen by the microwave sensor. If we allow all the multiple reflections to remain, we have a better fit to the emissivity given by the Wentz functions (see Fig. 5). The treatment of multiple surface interactions in this manner is acceptable



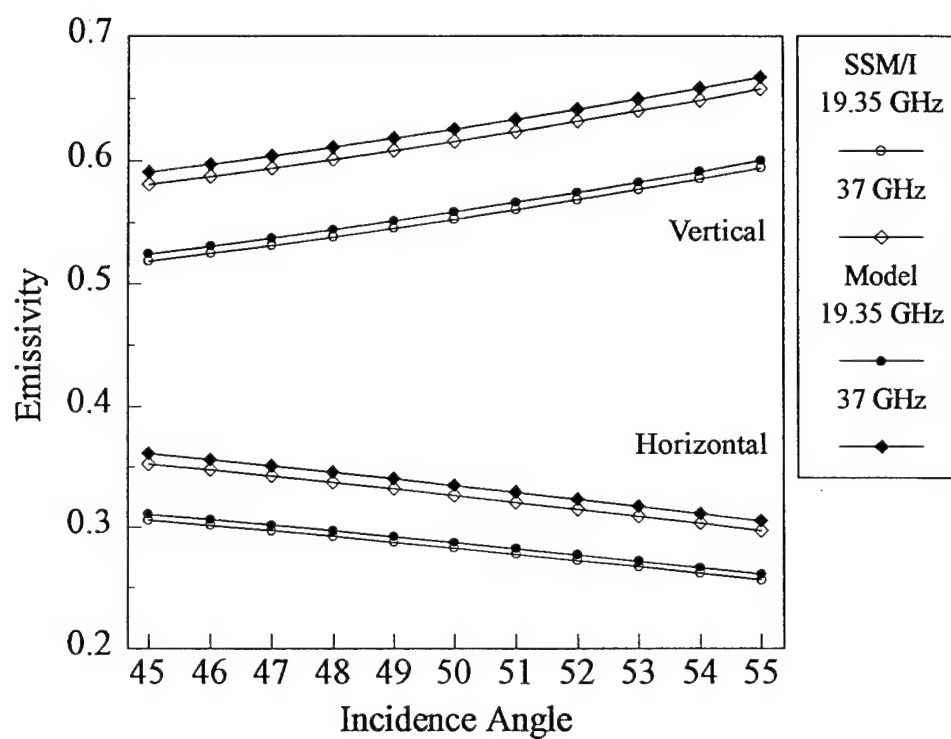


Fig. 2. Incidence angle dependence of the model and the SSM/I function for surface emissivity.

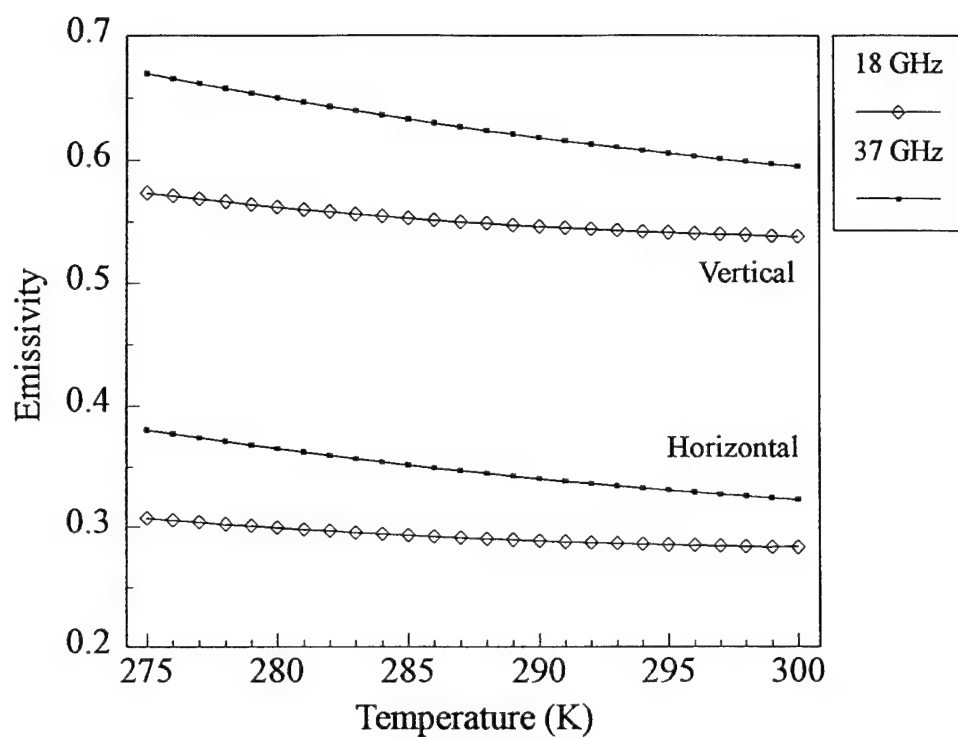


Fig. 3. The sea surface temperature dependence of the sea surface emissivity model.

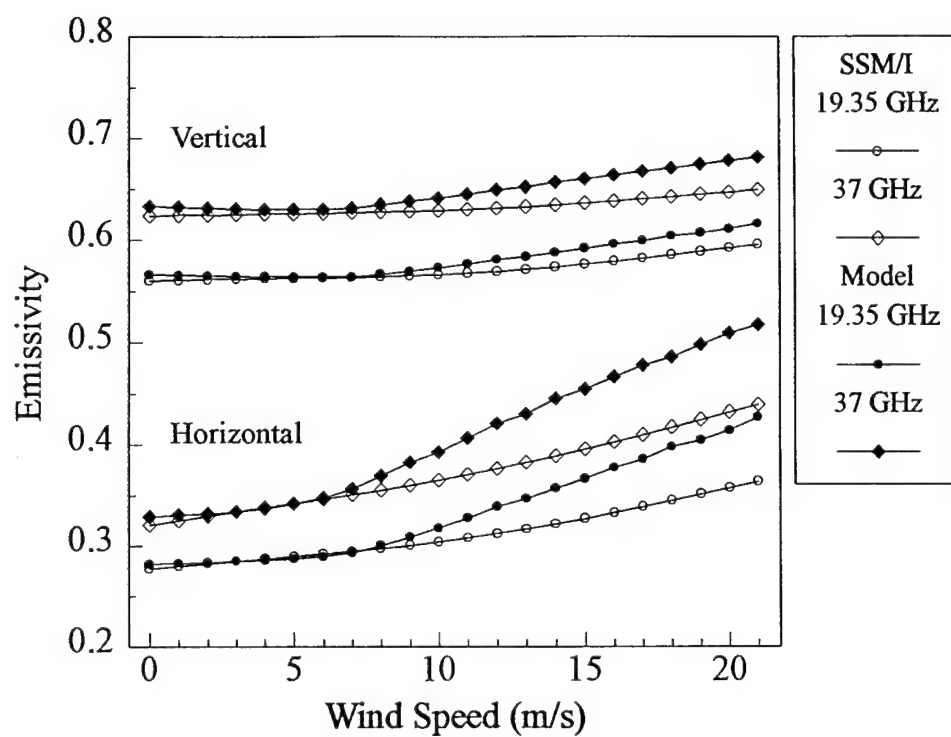


Fig. 4. Wind speed dependence of the model and the SSM/I function.

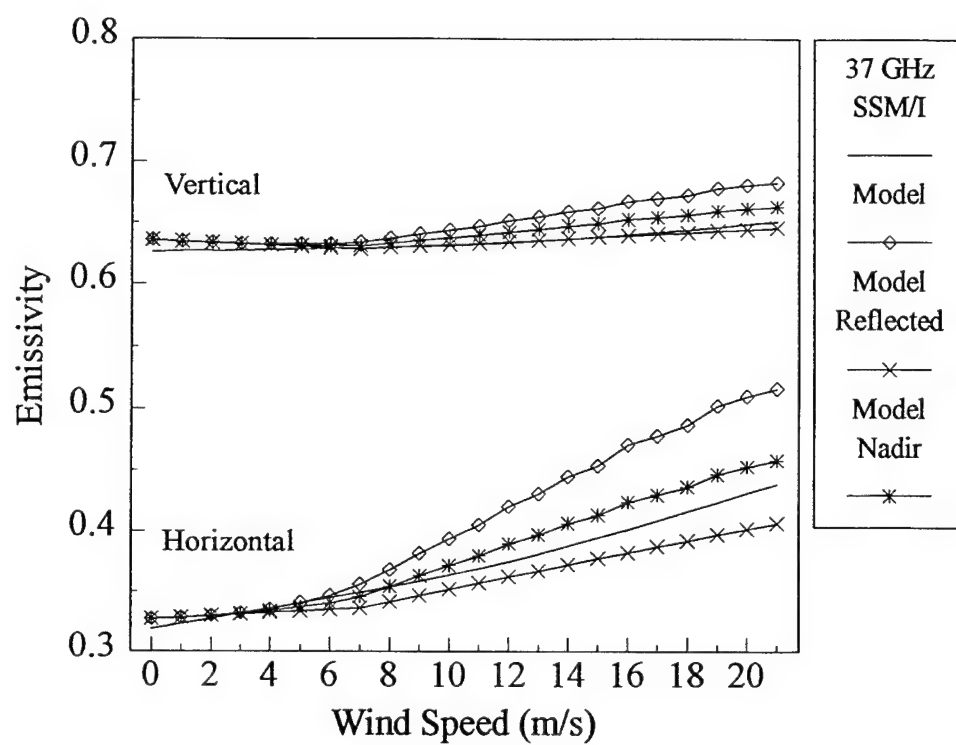


Fig. 5. The treatment of multiple reflections in the model.

because if a ray is reflected out of the field of view, on the average, another ray is reflected back into the field of view. Also shown in Fig. 5 is the case where the multiple reflections are modeled as though the second surface interaction were at nadir. The case where all the radiation is reflected back into the view path follows just below the emissivities given by the Wentz functions. Therefore, this case is used in the model for the rest of the calculations.

Next, the roughness parameter of the model is compared to the roughness given by the Wentz functions. The roughness parameter ( $F$ ) is defined as

$$F = \frac{R_h}{R_v} = \frac{1-E_h}{1-E_v} \quad (21)$$

where  $R_h$  is the horizontal reflectivity,  $E_h$  is the horizontal emissivity,  $R_v$  is the vertical reflectivity, and  $E_v$  is the vertical emissivity. This parameter does not have any foam effect because foam has no polarization characteristics (Wilheit 1979). From the roughness plots at high wind speeds, more roughness is needed at 37 GHz and at frequencies below 19.35 GHz less roughness is needed (see Fig. 6).

Roughness in the model is adjusted by changing the variance in the mean square slopes of the facets. At a wind speed of 20 m/s, the 6.6, 10.7, 18, and 37 GHz channels need a change of -10.3%, -6.8%, -1.3%, and 32% in roughness respectively. This change is needed even after taking into account the change to the Cox and Munk variance made by Hollinger (1971). A line fit to the above data points yield a decrease in roughness below 16.6 GHz and an increase above 16.6 GHz (see Fig. 7). The crossover at 16.6 GHz suggests that Hollinger overestimates the slope variance below this point and

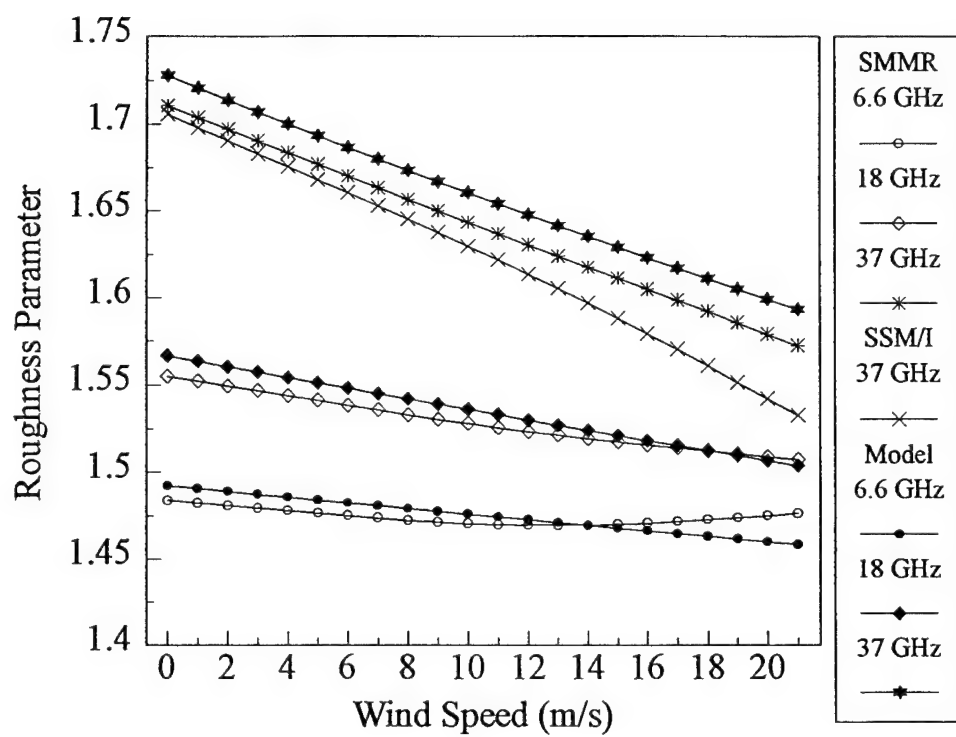


Fig. 6. Plots of the roughness parameter for SMMR frequencies.

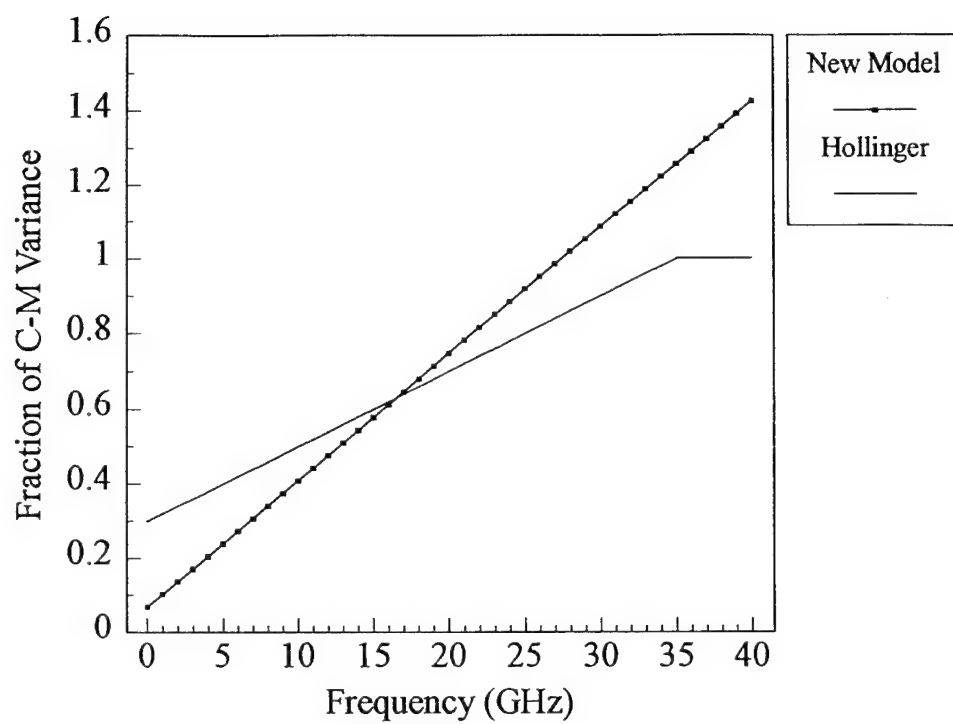


Fig. 7. A comparison of Hollinger's and the new model's Cox and Munk variance adjustment.

underestimates the variance above this point. The resulting equation is added to the reduction of the Cox and Munk variance as found by Hollinger. The new adjustment to the Cox and Munk variance is given by the following expression:

$$0.06852 + 0.03393 \times f \quad (22)$$

where  $f$  is the frequency in GHz. This adjustment to the roughness fits the data better and closer to the roughness given by the Wentz SSM/I 37 GHz function (see Fig. 8). The new expression yields a 132% of the Cox and Munk variance at 37 GHz. Guillou *et al.* (1995) have suggested that at high frequencies the sea surface roughness may be as high as 2.5 times the Cox and Munk roughness. At frequencies above 40 GHz, the model uses 100% of the Cox and Munk variance. At the 40 GHz cutoff, the model uses 143% of the Cox and Munk variance. This cutoff is chosen because not much data are available above this frequency.

Having a good estimate of the roughness, we can now make an adjustment to the foam contribution. The emissivity is now computed without foam using the model. This emissivity is subtracted from the total emissivity obtained from the Wentz functions. The remaining emissivity is considered to be from foam. The residuals should be zero at 0 m/s wind speed, but they are not (see Fig. 9). The model emissivities are considered to be more accurate because the computed smooth surface emissivities are based on the Lane and Saxton dielectric data rather than the Klein and Swift expression for the dielectric constant. Therefore, the offset at 0 m/s wind speed is subtracted from all wind speeds at each frequency. This adjusts for zero foam at 0 m/s wind speed (see Fig. 10).



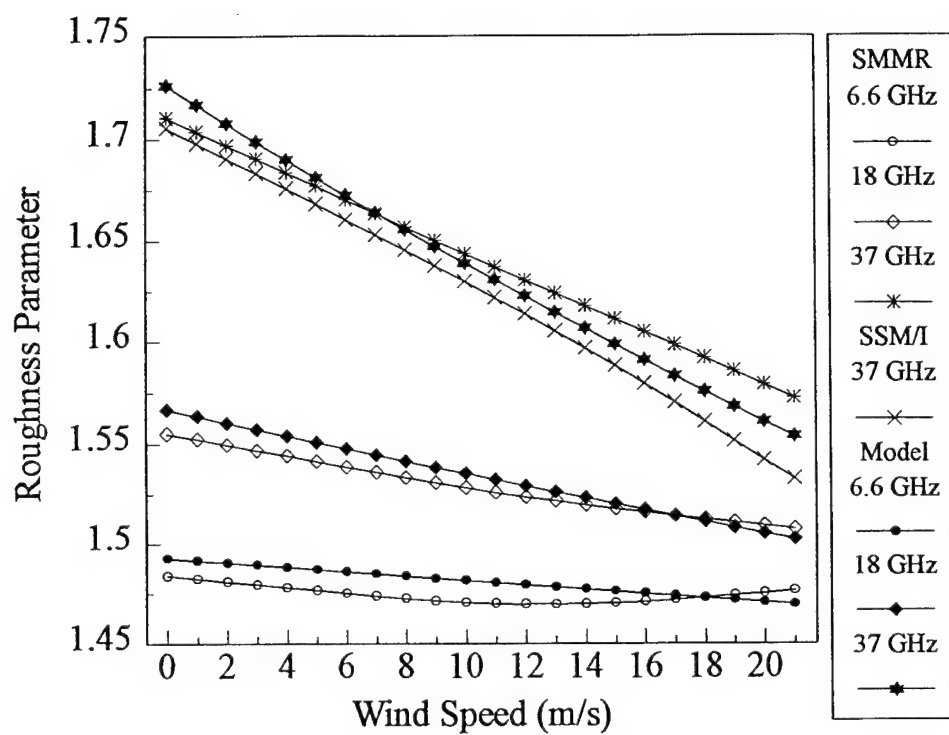
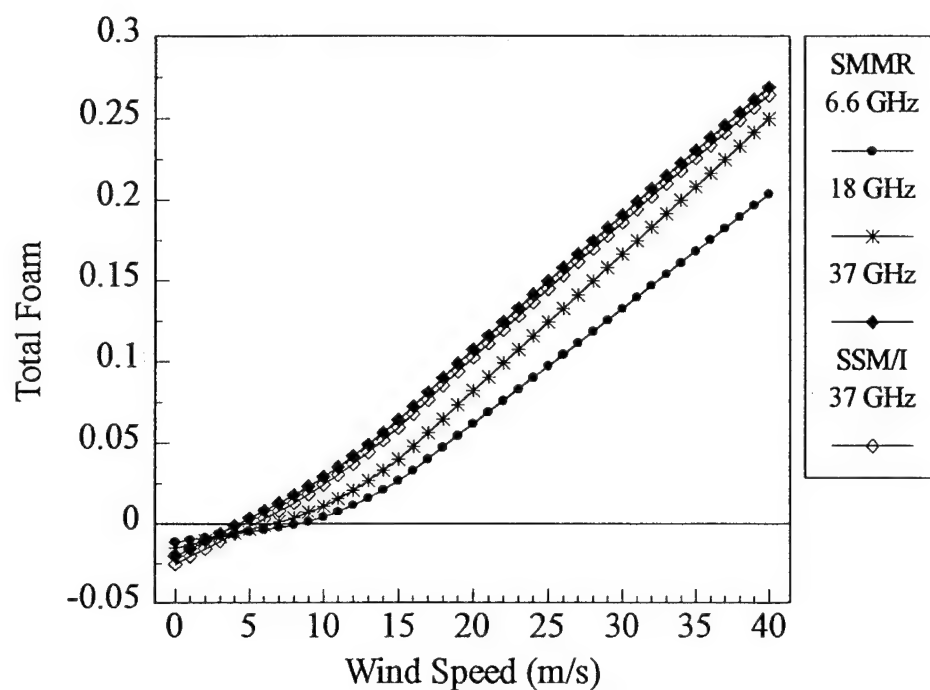
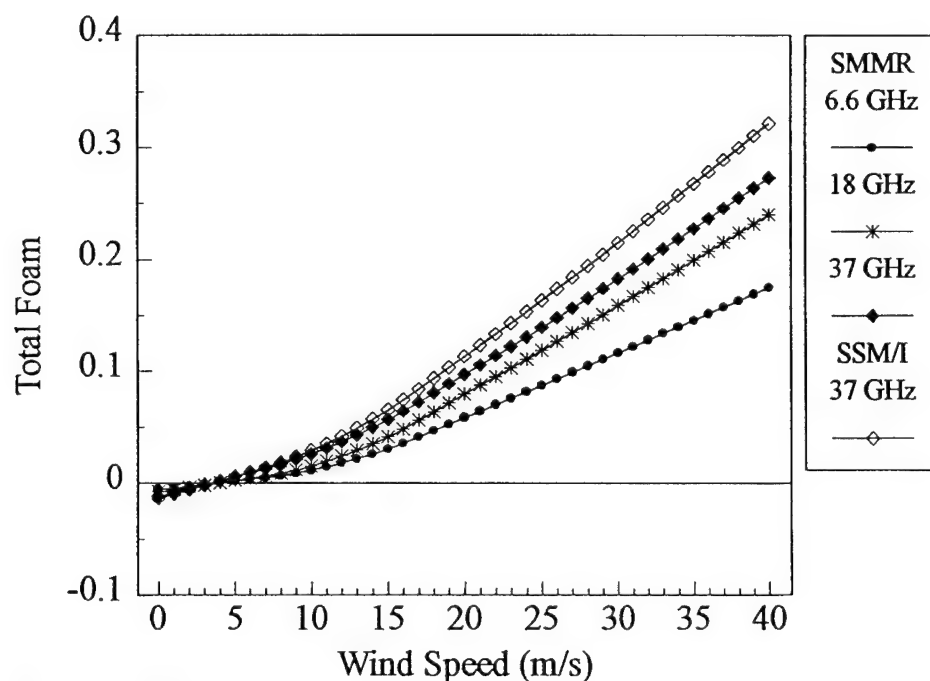


Fig. 8. Plots of the roughness parameter for SMMR frequencies after the variance adjustment.



Vertical Polarization



Horizontal Polarization

Fig. 9. Total foam effect (Wentz functions minus the new model's emissivities without the foam contribution).

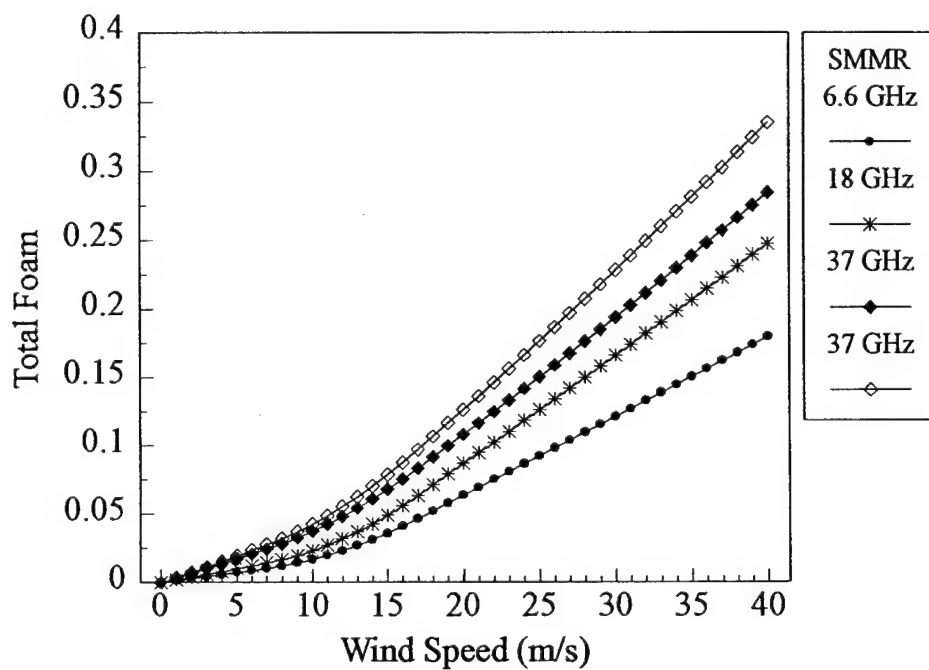
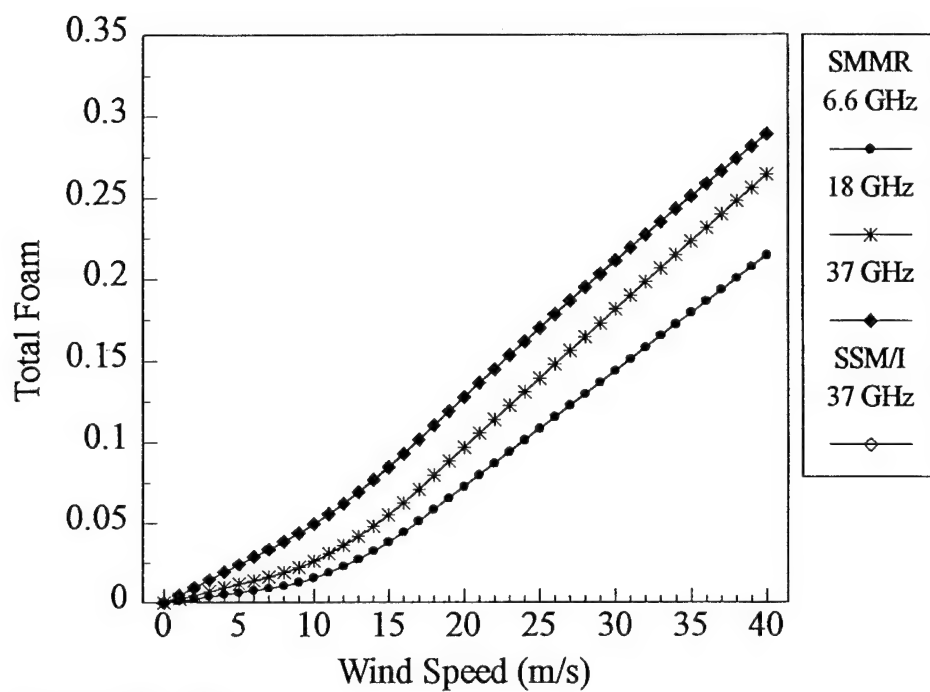


Fig. 10. Adjusted foam effect with zero foam at 0 m/s wind speed.

The graph of the residuals shows two linear segments; one below wind speeds of 7 m/s and one above 17 m/s. This result can be expected since Wentz developed the sea surface emissivity functions in this manner with respect to wind speed. He connected the two linear segments with a quadratic spline. In the same manner, a base function for the foam effect is developed which is only a function of wind speed (see Fig. 11). This function is chosen so that when it is subtracted from the 6.6 GHz horizontal and vertical channels the horizontal remainder stays positive and is close to the 6.6 GHz vertical values. The base function chosen is

$$0.0012 \times WS \quad WS \leq 7 \text{ m/s} \quad (23)$$

$$0.000195 \times WS^2 - 0.00153 \times WS + 0.009555 \quad 7 < WS < 17 \text{ m/s} \quad (24)$$

$$0.0051 \times WS - 0.04587 \quad 17 \leq WS \quad (25)$$

When subtracted from the total foam effect, this function reduces the bend in the foam contribution (see Fig. 12).

After the base function is subtracted from the foam contribution at each frequency and polarization, the remaining foam effect is a function of frequency and wind speed. To determine the frequency dependence, the remaining foam contribution is expressed as a fraction of the base function (see Fig. 13). From Fig. 13, the fractions of the base function remain fairly constant below 7 m/s and above 17 m/s; except in the 37 GHz channel. An average fraction is chosen for each of these segments at each frequency and polarization. At 37 GHz, the curvature to the fraction is due to atmospheric interference which makes the 37 GHz channel difficult to model. The 37 GHz emissivities from the Wentz SMMR

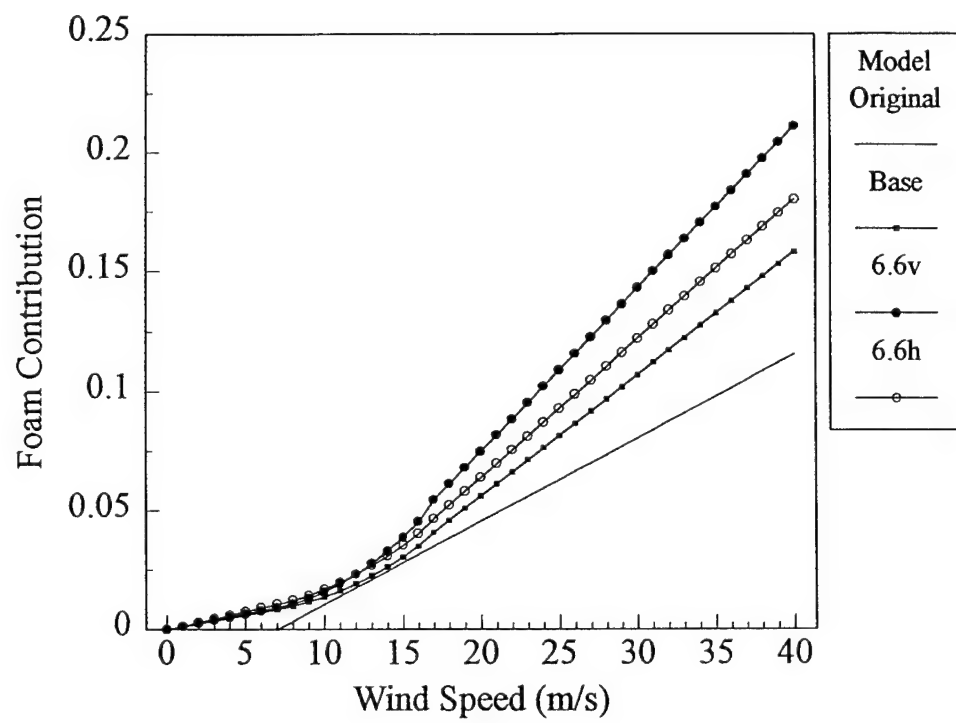
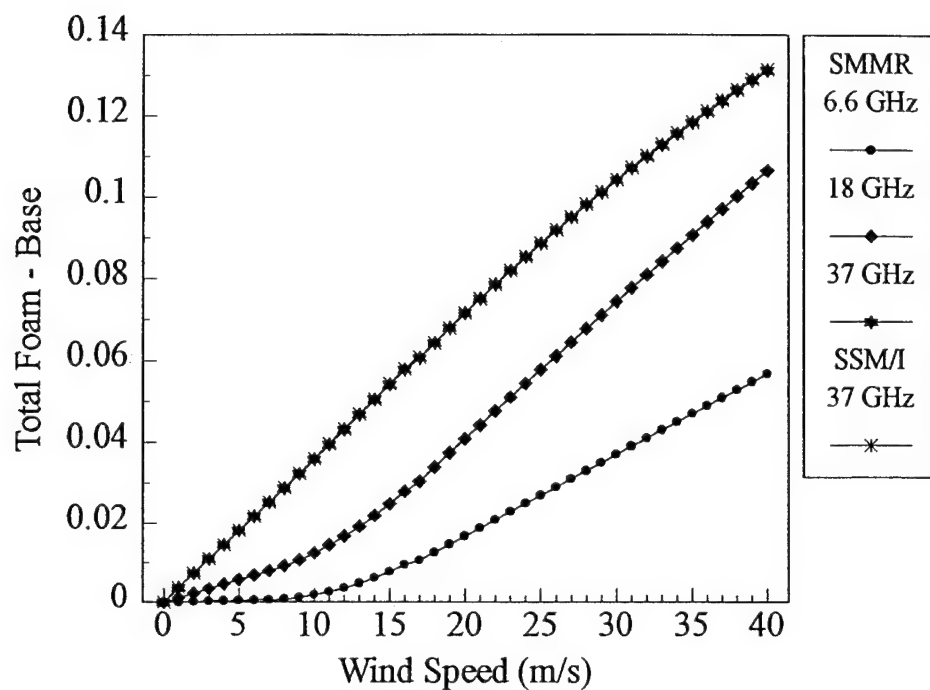
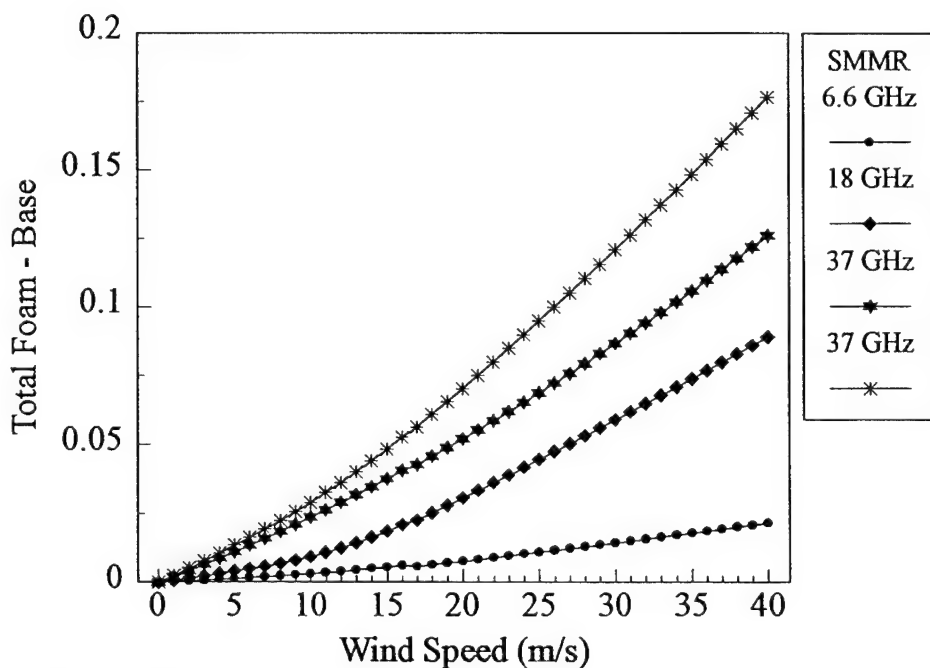


Fig. 11. Wind speed dependence of the foam effect.

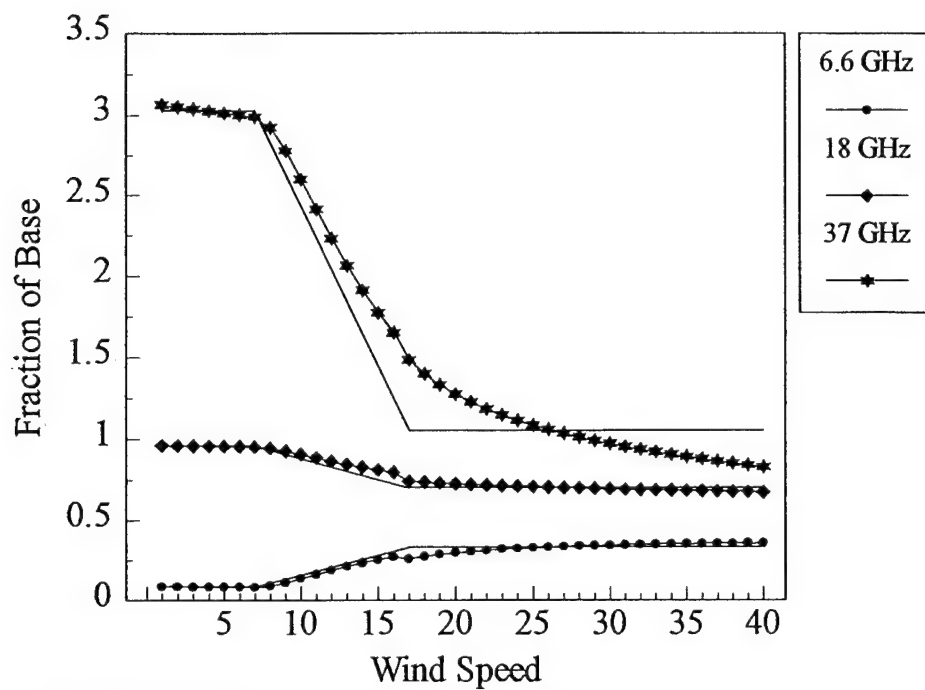


Vertical Polarization

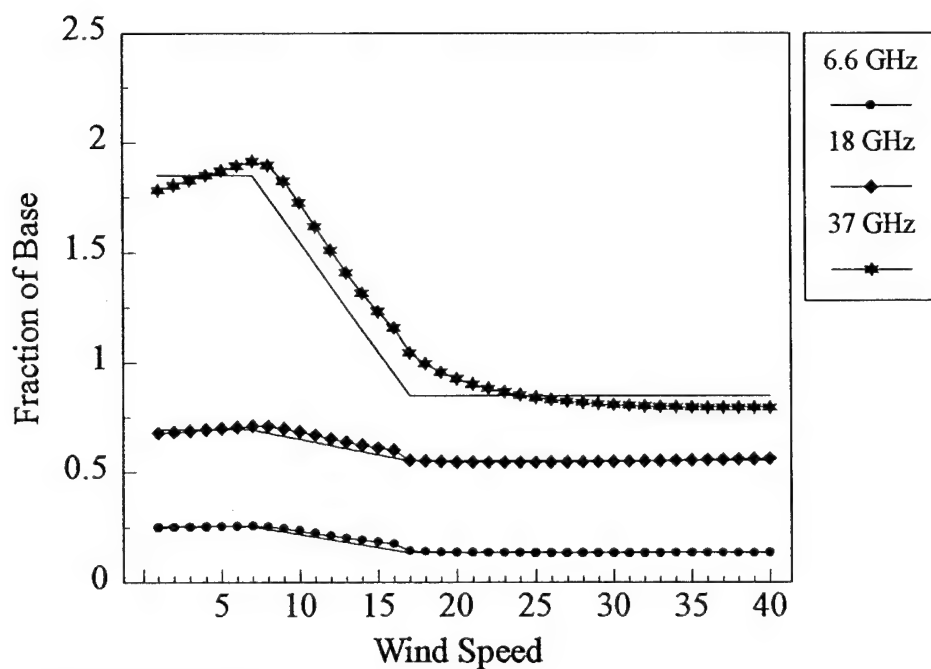


Horizontal Polarization

Fig. 12. The remaining foam contribution after the base function is subtracted from the total foam effect.



Vertical Polarization



Horizontal Polarization

Fig. 13. The remaining foam contribution expressed as a fraction of the base function (the straight line segments are the new functions for the remaining foam contributions).

and SSM/I functions do not even agree (see Fig. 14). The functions are not totally self-consistent because they are a best fit to the data. Also, there does not exist any data that would suggest that the 37 GHz foam fraction should behave differently than the foam fraction at the other frequencies. Therefore, an average fraction can be used for 37 GHz without much error. A polynomial is fit to the average fraction as a function of frequency for both horizontal and vertical polarizations (see Fig. 13). The resulting equations are in the form of

$$a_0 + a_1 \times f + a_2 \times f^2 + a_3 \times f^3 \quad (26)$$

where  $f$  is frequency (GHz). The  $a$  coefficients are in Table 4.

Between 7 m/s and 17 m/s, the remaining foam contribution is a function of frequency and wind speed. The function chosen is linear in wind speed and connects the constant fractions below 7 m/s and above 17 m/s at each frequency (see Fig. 13). The slopes of these connecting segments are different for each frequency and polarization. The slopes and intercepts of the connecting segments are calculated for each frequency and polarization. Next, polynomials are fit to the slopes and intercepts as a function of frequency. The slope and intercept equations are combined to form one equation; one for the horizontal polarization and one for the vertical polarization. The resulting equations are in the form of

$$b_0 + b_1 \times f + b_2 \times f^2 + b_3 \times f^3 + (c_0 + c_1 \times f + c_2 \times f^2) \times WS \quad (27)$$

This equation is valid for wind speeds between 7 and 17 m/s. The  $b$  and  $c$  coefficients are in Table 4.



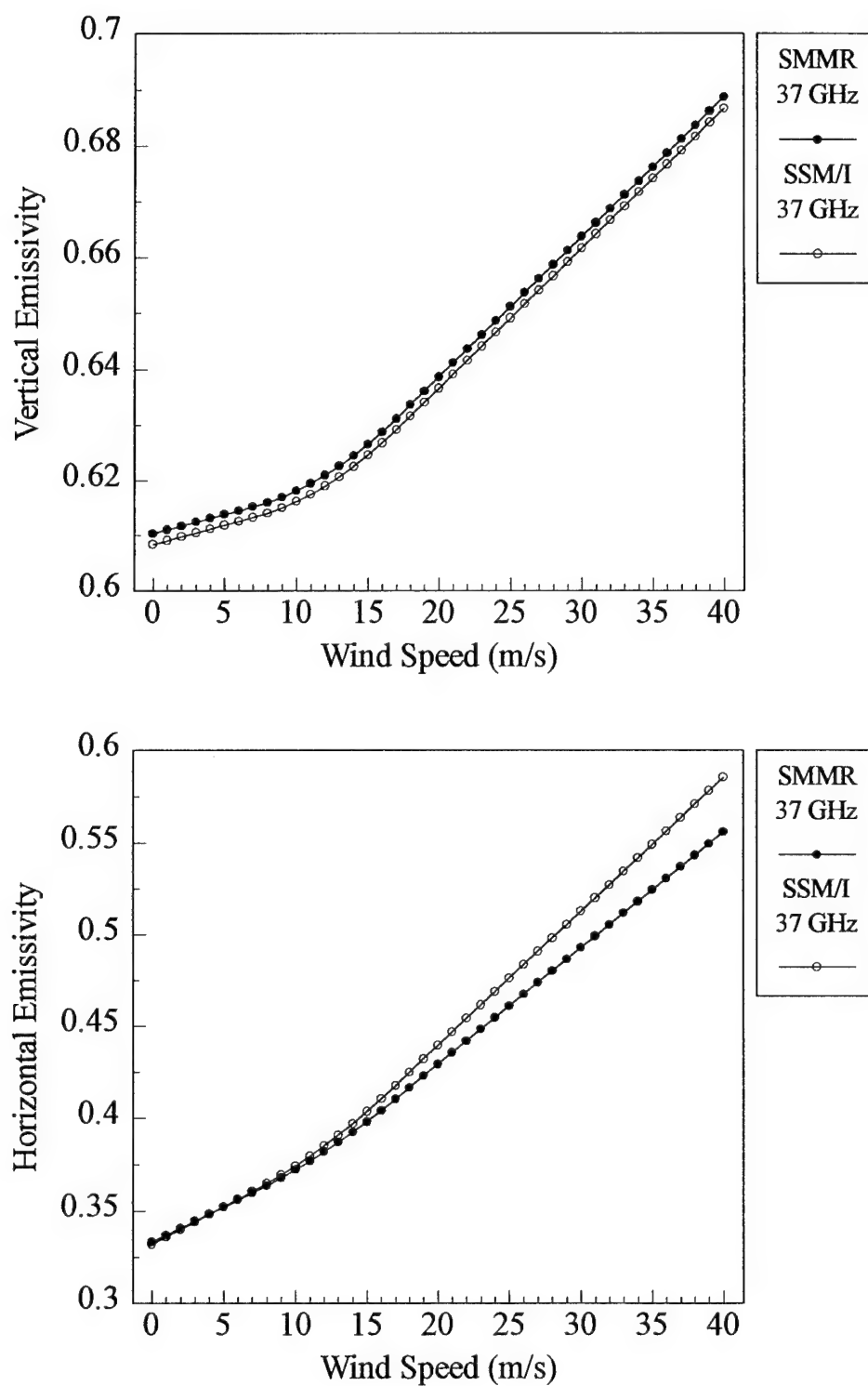


Fig. 14. A comparison of the 37 GHz emissivities from the SMMR and SSM/I functions.

TABLE 4. Coefficients for the frequency dependence equations of the foam effect.

	Horizontal	Polarization	Vertical	Polarization
	$\leq 7m/s$	$\geq 17m/s$	$\leq 7m/s$	$\geq 17m/s$
$a_0$	-0.36025	-0.58956	-0.7783	-0.3146
$a_1$	0.12506	0.1478	0.1643	0.1325
$a_2$	-0.0051709	-0.0062256	-0.005604	-0.005697
$a_3$	0.000092046	0.00008869	0.0001066	0.00008414
	$7 < WS < 17m/s$		$7 < WS < 17m/s$	
$b_0$	-0.1991		-1.103	
$b_1$	0.109		0.1866	
$b_2$	-0.004426		-0.005541	
$b_3$	0.00009429		0.0001223	
$c_0$	-0.02475		0.03423	
$c_1$	0.002654		-0.0006405	
$c_2$	-0.00012682		-0.0001519	

The overall frequency dependence of the foam effect is similar to frequency dependence given by Wilheit's foam function. His function is exponential in frequency and the new foam function is cubic in frequency. This new function is similar to Wilheit's function until approximately 17 GHz at which point it begins to increase (see Fig. 15). This increase in the function is needed to account for the larger foam effect seen at 37 GHz.

The overall wind speed dependence of the foam effect is similar to the base function (see Fig. 11). Also in Fig. 11, the wind speed dependence of Wilheit's function is seen. The new wind speed dependence of the foam effect is a smooth transition to increasing foam as the wind speed increases. The new foam function also has more foam at all wind speeds.

The resulting sea surface emissivity model is a big improvement over the old model. The new model's emissivity follow closely to the emissivities given by the Wentz functions (see Fig. 16). The emissivities from the new model are slightly offset from the emissivities given by the Wentz functions. The offset is by design because the computed emissivities at 0 m/s wind speed are different. The emissivities given by the new model follow the form of the Wentz functions. The emissivities from the new model are within 2% of the emissivities from the Wentz functions.

The fortran source code for the new sea surface emissivity model is given in Appendix A. This code is used to produce the total sea surface emissivity.

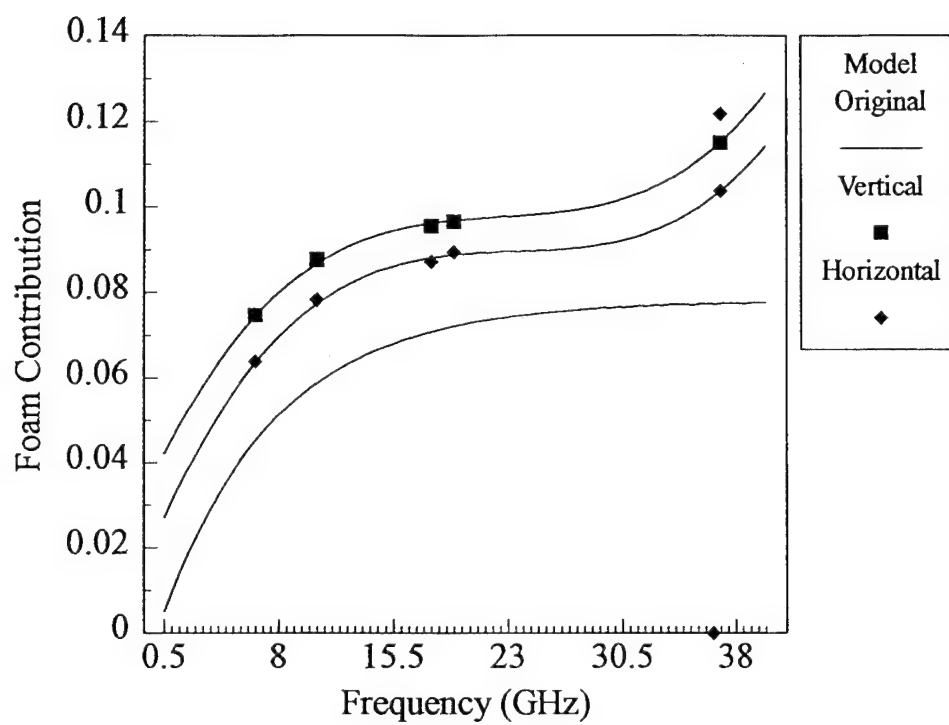


Fig 15. Frequency dependence of the foam effect at 20 m/s wind speed.

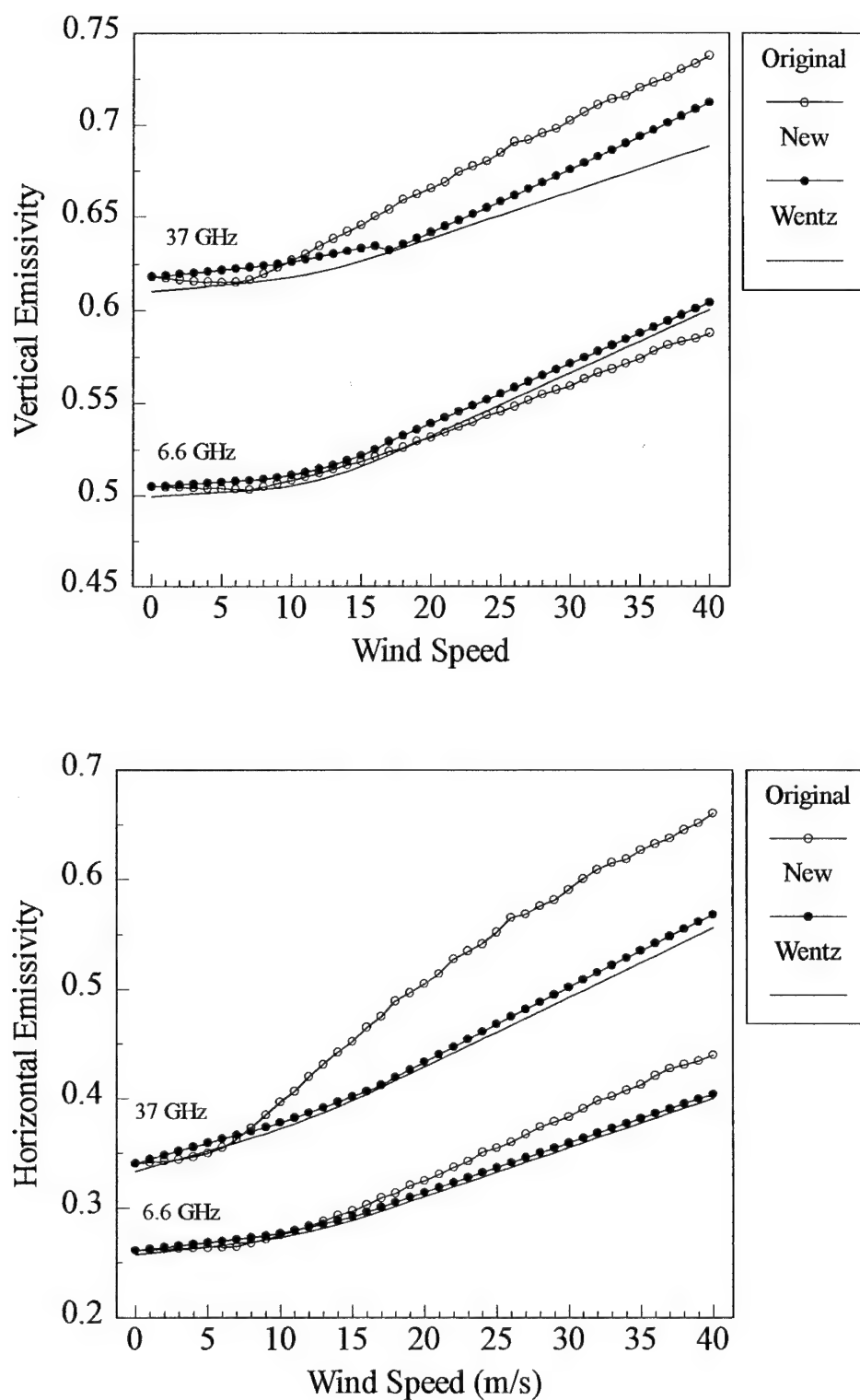


Fig. 16. Emissivities from the new model and the Wentz functions.

#### 4. CONCLUSION

Several changes are made to Wilheit's sea surface emissivity model. The first change to the model is to the model's treatment of multiple reflections. Multiple reflections are now treated as if the radiation were reflected back into the view path of the microwave sensor. This change lowered the emissivity of the sea surface; which is more representative of observations without sea foam. The second change is made to the sea surface roughness parameter. An increase in roughness is needed at frequencies above 16.6 GHz and a decrease below 16.6 GHz. The roughness is increased to 132% of the Cox and Munk roughness at 37 GHz and 30% of the roughness at 6.6 GHz. The last change to the model is in the treatment of sea foam. The foam effect is now a smooth transition to increasing foam as the wind speed increases; instead of being switched on at 7 m/s. These changes yield an improved sea surface model whose emissivities fall within 2% of the emissivities from the Wentz functions.

While the Wentz sea surface emissivity functions are adequate for the SMMR and the SSM/I frequencies and incidence angles, there remains a need for a more general model for all frequencies and incidence angles. The new model does not have these limitations. Therefore, it can be used to simulate brightness temperatures for other frequencies and incidence angles.

## REFERENCES

- Chang, A. T. C., and T. T. Wilheit, 1979: Remote sensing of atmospheric water vapor, liquid water, and wind speed at the ocean surface by passive microwave techniques from the Nimbus 5 satellite. *Radio Sci.*, **14**, 793-802.
- Cox, C., and W. Munk, 1955: Some problems in optical oceanography. *J. Marine Res.*, **14**, 63-78.
- Griffiths, D. J., 1989: *Introduction to Electromagnetics (2nd Ed.)*. Prentice Hall, 532 pp.
- Guillou, C., S. J. English, C. Prigent, and D. C. Jones, 1995: Passive microwave airborne measurements of the sea surface response at 89 and 157 GHz. Submitted to *J. Geophys. Res.* Personal collection of, D. J. Kohn.
- Hollinger, J. P., 1971: Passive microwave measurements of sea surface roughness. *IEEE Trans. Geosci. and Remote Sensing*, **GE-9**, 165-169.
- Klein, L. A., and C. T. Swift, 1977: An improved model for the dielectric constant of sea water at microwave frequencies. *IEEE Trans. Antennas Propagat.*, **AP-25**, 104-111.
- Lane, J. A., and J. A. Saxton, 1952: Dielectric dispersion in pure polar liquids at very high radio-frequencies I. Measurements on water, methyl and ethyl alcohols. *Proc. Roy. Soc., London A*, **214**, 400-408.
- Nordberg, W., J. Conaway, D. B. Ross, and T. Wilheit, 1971: Measurements of microwave emission from a foam-covered, wind-driven sea. *J. Atmos. Sci.*, **28**, 429-435.
- Ross, D. B., V. Cardone, 1974: Observations of oceanic whitecaps and their relation to remote measurements of surface wind speed. *J. Geophys. Res.*, **79**, 444-452.
- Shutko, A., 1978: Report on Soviet progress in microwave radiometry of the ocean's surface. *IUCRM Colloquium on Passive Radiometry of the Ocean's Surface*. Patricia Bay, B. C., Canada.
- Smith, P. M., 1988: The emissivity of sea foam at 19 and 37 GHz. *IEEE Trans. Geosci. and Remote Sensing*, **26**, 541-547.
- Wentz, F. J., 1983: A model function for ocean microwave brightness temperatures. *J. Geophys. Res.*, **88**, 1892-1908.

- \_\_\_\_\_, L. A. Mattox, and S. Peteherych, 1986: New algorithms for microwave measurements of ocean winds applications to SEASAT and the special sensor microwave imager. *J. Geophys. Res.*, **91**, 2289-2307.
- \_\_\_\_\_, 1992: Measurement of oceanic wind vector using satellite microwave radiometers. *IEEE Trans. Geosci. and Remote Sensing*, **30**, 960-972.
- Wilheit, T. T., 1979: A model for the microwave emissivity of the ocean's surface as a function of wind speed. *IEEE Trans. Geosci. Electron.*, **GE-17**, 244-249.
- \_\_\_\_\_, and A. T. C. Chang, 1980: An algorithm of ocean surface and atmospheric parameters from the observations of the scanning multichannel microwave radiometer. *Radio Sci.*, **15**, 525-544.
- Williams, G. F., 1971: Microwave emissivity measurements of bubbles and foam. *IEEE Trans. Geosci. Electron.*, **GE-9**, 221-224.



## APPENDIX A

SUBROUTINE ROUGH(F,ANGLE,TEMP,PPT,WS,VERT,HORIZ)

```

C
C *****
C * THIS SUBROUTINE COMPUTES VERTICAL AND HORIZONTAL      *
C * EMISSIVITIES FROM COX AND MONK AT 20M WHERE           *
C *                                                         *
C * F-FREQUENCY IN GHz                                     *
C * ANGLE-INCIDENCE ANGLE IN RADS                          *
C * TEMP-TEMP IN K                                         *
C * PPT-SALINITY IN PARTS PER THOU.                       *
C * WS-WIND SPEED IN M/S                                   *
C * VERT- VERTICAL POLARIZATION                           *
C * HORIZ-HORIZONTAL " " " " "                            *
C *****
C
C Variance of sea surface roughness given by Cox and Munk. And changes to the
C variance as given by the new model.
C
VAR=0.003+4.80*WS/1000.
IF (F .LE. 40.0) VAR=VAR*(0.06852+0.03393*F)
T=TEMP
VERT=0.
HORIZ=0.
YNORM=0.
SIG=SQRT(VAR)
STEP=SIG/10.
SA=SIN(ANGLE)
CA=COS(ANGLE)
C
C Calculation of the relaxation time (TAU) of the dielectric constant
C of sea water (Lane and Saxton)
C and International Critical Tables conductivity data
C
S=PPT/58.4
XLAM=51.-4.835*S+1.728*(T-273.)-0.2037*S*(T-273.)
IF(S.GT.1.) XLAM=XLAM-0.35/S
ES=190.-81*S+38*S*S-(03.75-2.*S+S*S)*T/10.
T1=0.00199*EXP(2140/T)/T
T2=0.00243*EXP(2060/T)/T-T1
T3=0.00324*EXP(1968/T)/T-T1
TAU=T1+(4.*T2-T3)*S+(2.*T3-4.*T2)*S*S
C

```

```

C  TAU in nanoseconds, F in GHz, T in deg K, S is salinity
C  Dielectric constant Calculation
C  RPE, XIPE are the real and imaginary parts of the dielectric constant respectively
C
  X=6.283*F*TAU
  EZ=4.9
  RPE=EZ+(ES-EZ)/(1.+X*X)
  XIPE=(ES-EZ)*X/(1.+X*X)+1.8*XLAM*S/F
C
C  Taking the square root of the complex dielectric constant
C  to get the complex index of refraction
C  RPN, XIPN are the real and imaginary parts of the index of refraction respectively
C
  XMODE=SQRT(RPE**2+XIPE**2)
  XMODN=SQRT(XMODE)
  ARGN=0.5*ATAN(XIPE/RPE)
  RPN=XMODN*COS(ARGN)
  XIPN=XMODN*SIN(ARGN)
C
C  Calculates the emissivity contribution of each facet and sums up the emissivities
C
  DO 100 J=1,61
  DO 100 KK=1,31
  K=KK-1
  ZX=STEP*(J-31)
  ZY=STEP*K
C
C  The distribution used the one used by Cox and Munk
C
  WEIGHT=EXP(-((J-31)**2+K*K)/100.)
  IF(KK.EQ.1) WEIGHT=WEIGHT/2.
C
C  Facet hidden from view
C  RDN is the dot product between the incoming ray and facet normal
C
  RDN=CA+ZX*SA
  IF (RDN .LT. 0.) GO TO 100
C
C  STP is the sine squared of above angle calculated by 1-cosine**2
C
  STP=(SA*SA+ZX*ZX+ZY*ZY-(ZX*SA)**2-2.*ZX*SA*CA)/(1+ZX*ZX+ZY*ZY)
  SI=SQRT(STP)
  IF (SI .LT. 0.001) SI=0.001
  EM=ZY*ZY/(1.+ZX*ZX+ZY*ZY)

```

```

EM=EM/(SI*SI)
IF (SI .LT. 0.00101) EM=.5
CI=SQRT(1.-SI*SI)
WEIGHT=WEIGHT*CI
YNORM=YNORM+WEIGHT
C
C Projection of facet in view direction
C Squaring the complex index of refraction and finds the complex conjugate
C of the squared index of refraction
C
AN2=RPN**2+XIPN**2
SRR=RPN*SI/AN2
SRI=-XIPN*SI/AN2
XMOD=((1.-SRR**2+SRI**2)**2+(2.*SRR*SRI)**2)**0.25
ARG=-0.5*ATAN(2.*SRR*SRI/(1.-SRR**2+SRI**2))
CRR=XMOD*COS(ARG)
CRI=XMOD*SIN(ARG)
C
C Calculates the reflected emissivity with the Fresnel equations
C
RH=((SI*CRR-CI*SRR)**2+(SI*CRI-CI*SRI)**2)/((SI*CRR+CI*SRR)**2+
&(SI*CRI+SRI*CI)**2)
RV=RH*((CI*CRR-SI*SRR)**2+(CI*CRI-SI*SRI)**2)/((CI*CRR+SI*SRR)**2+
&(CI*CRI+SRI*SRI)**2)
C
HORIZ=HORIZ+WEIGHT*((1.-EM)*(1.-RH)+EM*(1.-RV))
VERT=VERT+WEIGHT*((1.-EM)*(1.-RV)+EM*(1.-RH))
C
100 CONTINUE
C
HORIZ=HORIZ/YNORM
VERT=VERT/YNORM
C
C Adds foam effect
C
IF (WS .LE. 7.0) THEN
C
FOAM=0.0012*WS
FOAMV=FOAM+FOAM*(-0.7783+0.1643*F-0.005604*F*F+0.0001066*F*F*F)
FOAMH=FOAM+FOAM*(-0.36025+0.12506*F-0.0051709*F*F+
&0.000092046*F*F*F)
C
ELSEIF ((WS .GT. 7.0) .AND. (WS .LT. 17.0)) THEN
C

```

```
FOAM=0.000195*WS*WS-0.00153*WS+0.009555
FOAMV=FOAM+FOAM*(-1.103+0.1866*F-0.005541*F*F+
&0.0001223*F*F*F+(0.03423-0.0006405*F-0.000141519*F*F)*WS)
FOAMH=FOAM+FOAM*(-0.1991+0.109*F-0.004426*F*F+
&0.00009429*F*F*F+(-0.02475+0.002654*F-0.00012682*F*F)*WS)
C
ELSE
C
FOAM=0.0051*WS-0.04587
FOAMV=FOAM+FOAM*(-0.3146+0.1325*F-0.005697*F*F+0.00008418*F*F*F)
FOAMH=FOAM+FOAM*(-0.58956+0.1478*F-0.0062256*F*F+0.00008869*F*F*F)
C
ENDIF
C
HORIZ=FOAMH+(1.-FOAMH)*HORIZ
VERT =FOAMV+(1.-FOAMV)*VERT
RETURN
END
```

## VITA

David Jacob Kohn was born in St. Joseph, Michigan and attended the Lakeshore Public School system. He entered ROTC while attending Michigan Technological University in 1985. He graduated from Michigan Technological University with a Bachelor of Science degree in Metallurgical Engineering in 1987. Upon graduation, he was commissioned as a 2nd lieutenant in the United States Air Force. His first assignment was to Texas A&M University to complete the Basic Meteorology Program. After completing the program, he was sent to Bitburg Air Base, Germany as the Wing Weather Officer. His next assignment was to Fort Hood Army Installation, Texas as a Staff Weather Officer. While stationed at Fort Hood, he applied and was accepted into the Air Force Institute of Technology's Masters program and was sent to Texas A&M University. There he became a member of the Microwave Remote Sensing Group and focused his research on modeling the sea surface emissivity.

Kohn married the former Lara Lynn Mattson in November 1992. They have one son, Matthew, born 1 April 1995.

Correspondence may be sent to: 9728 Hills Rd., Baroda, Michigan 49101.